

Engine Block Vibrations – An Indicator of Knocking in the SI Engine

Antonio Joseph V. K.

Research Scholar
Department of Mechanical Engineering
School of Engineering
Cochin University of Science and
Technology
Kalamassery, Kerala
India

Gireeshkumaran Thampi

Professor
Department of Mechanical Engineering
School of Engineering
Cochin University of Science and
Technology
Kalamassery, Kerala
India

The factors influencing the onset of knocking have a significant impact on how well a SI engine performs. Hence, the efficacy in determining the onset and controlling of knock is a key factor in improving the SI engine's performance. This paper provides insight into the role of engine block vibrations in determining the occurrence of knock using Empirical Mode Decomposition and Short-Time Fourier Transform. To comprehend the behaviour of vibration amid normal combustion and knocking conditions, the engine block vibration signals are analyzed and compared with the in-cylinder pressure fluctuations. The features of knock are extracted from the engine block vibration signals using Empirical Mode Decomposition. The first Intrinsic Mode Function (IMF) thus obtained is used to generate the Hilbert spectrum for detecting the occurrence of knock. Similarly, Short-Time Fourier Transform is also performed on the first IMF to obtain the spectrogram. The findings demonstrate unequivocally that higher frequency variations are produced when knock occurs. These results also indicate that the combination of Empirical Mode Decomposition and Short-Time Fourier Transform can be used effectively for determining the occurrence of knock.

Keywords: Spark Ignition Engine, Knocking, Empirical Mode Decomposition, Hilbert Transform, Short-time Fourier Transform, Spectrogram.

1. INTRODUCTION

The stringent emission norms and the issues pertaining to climatic changes had made the researchers consider alternate fuels or improving the performance of conventional fueled engines. The studies show that the performance of the SI engines improves with the compression ratio; however, it results in knocking above a particular value, called Highest Useful Compression Ratio (HUCR) [1]. Hence, the improvement in the performance of SI engines will not be possible beyond a certain limit. However, the knock could be suppressed to a certain extent by reducing the in-cylinder temperature [1]. Cooled Exhaust Gas Re-circulation, water injection system, emulsified fuel, etc., could be used to extend the HUCR. Further improvement in the performance could be possible only if there is a possibility of real-time monitoring and control of SI engine knocking. Real-time SI engine knock suppression may be accomplished with cooled EGR [2]. However, the effectiveness in controlling the SI engine knock and improvement in the performance of an engine depends on how accurately we can predict the occurrence of knock. Many studies are available for predicting the occurrence of knock; based on the fuel octane number, ignition timing, in-cylinder pressure, temperature, the air-fuel ratio, etc. [3-6]. Due to the complexity, these studies failed to be efficiently employed for the real-time detection of knock. This leads

to the study of the behavior of various parameters that may be affected during the occurrence of a knock. Nanofluids were utilized as the coolant by Ollivier *et al.* [7] to explore the transient temperature fluctuations that occurred during the onset of knock. To amplify the transient temperature fluctuations, grooves facing the coolant flow were added to the cylinder liner [7]. This method could effectively detect the occurrence of knock. However, the time lag caused during the occurrence of temperature fluctuations and its analysis to confirm the knock makes it unfit for real-time monitoring and control of knock.

In-cylinder pressure, acoustic signals, and engine block vibrations are used by many researchers for the detection and analysis of knock [2, 8, 9]. The acoustic signals captured from the engine consist of noise, which requires proper analysis before extracting the features of knock. There are many methods for denoising the signals; among them, wavelets are found to be effective [8, 10, 11]. Also, there are various mathematical tools for analyzing denoised signals, including the Fourier transform, Wavelet transform, Empirical Mode Decomposition (EMD), etc. [12-18]. Furthermore, there are many variations and extensions of these models for extracting the features from the signals more efficiently and accurately [2, 9, 19, 20, 21]. Standard Fourier and Wavelet approaches use predefined functions as the basis for analyzing the signals [13, 22]. The Fourier analysis could be done only if there is at least one full wave oscillation of a sine or cosine wave to obtain the local frequency [13]. Therefore, the instantaneous frequency cannot be calculated for non-stationary data that changes the frequency now and then. Wavelet analysis could provide physically meaningful interpretations more accurately to only linear signals

Received: October 2022, Accepted: June 2023

Correspondence to: Antonio Joseph V K, Department of Mechanical Engineering, Cochin University of Science and Technology, Kerala, India

E-mail: antonioswas@gmail.com

doi: 10.5937/fme2303396K

© Faculty of Mechanical Engineering, Belgrade. All rights reserved

FME Transactions (2023) 51, 395-403 396

[13]. However, discrete wavelets could overcome this to a certain extent. Wavelets can be used to resolve inter-wave frequency modulations having a gradual frequency variation. However, it cannot be used to resolve intra-wave frequency modulations. This is because the basic wavelets have a length of 5.5 waves [13]. Therefore, the accuracy of the analysis depends on the stationarity, linearity, and length of the signal [13]. Unfortunately, the signals obtained from the SI engine are non-stationary and non-linear. Therefore, instead of Fourier Transform and Wavelet Transform, EMD is preferred in association with the Hilbert Spectrum analysis [13, 23]. However, because of mode mixing in EMD, there can be a probability that the knock's characteristics will be distributed over many Intrinsic Mode Functions (IMFs). This can be overcome by an improved version of EMD named Ensemble Empirical Mode Decomposition (EEMD). In this, the Mode mixing will be likely to be substantially less because the mean IMFs generated via EEMD will fall within the natural dyadic filter windows [20].

To reduce the effect of noise in the analysis, we can use in-cylinder pressure that could deliver important information about knock with less noise compared to the acoustic signals. However, the process is not economical since it requires pressure measuring devices in all the cylinders for capturing the in-cylinder pressure. Also, the analysis is more complicated since the number of signals captured depends on the number of cylinders in an engine and should be processed in parallel. However, many works were done for the real-time detection of knock using the in-cylinder pressure. Kim [24] used EEMD and Wavelet Packet Decomposition to analyze the in-cylinder pressure signals to categorize the cycles as knock and non-knock using the machine learning algorithm. Since knock produces high-frequency pressure fluctuations, Ofner *et al.* [25] developed 1-D Convolutional Neural Network that could capture the frequency-dependent features for identifying the knocking cycles.

Another source of signals bearing knock characteristics is the vibration signals obtained from the cylinder block. Accelerometers mounted on the cylinder block could capture the vibration. However, the vibration signals, thus obtained, contain noise since there are lots of vibrations occurring in other parts of the engine as well. Studies show that the amplitude of filtered vibration signals could be used for detecting the occurrence of knock and even for developing a knock index to classify the knock [26]. Ismail *et al.* [27] used a statistical approach to determine the occurrence of knock by comparing it with the knock index calculated using the engine block vibrations and the knock threshold. The vibration signal captured from the engine block contains the signals generated by all the moving parts in the engine. Also, there may be many external factors that contribute to the engine block vibrations in a running vehicle. Studies show that changes in the engine's working parameters affect the vibrations produced by the engine [28-30]. These changes are significant, and even significant variations are observed in the other parts of the vehicle due to these vibrations [28-30]. Hence, the data solely depending on the amplitude of the vibration signals may fail to determine

the occurrence of knock as well as to classify the knock based on its intensity. However, the engine block vibration analysis finds application in (i) detecting the malfunctioning of the moving parts, (ii) determining the engine performance, and (iii) designing the other parts of the vehicles [28-30]. The location at which the vibration signals are captured, as well as the methods adopted for analyzing the signals, are different for each purpose. Hence, research is going on to identify the most accurate and simple methods for each purpose.

In this work, the in-cylinder pressure and denoised vibration signals are analyzed to extract the features of knock. The signals are decomposed using EMD, even though there are many improved models like EEMD [9, 20], Complementary Ensemble Empirical Mode Decomposition [31], etc. This is due to the better adaptability of EMD in decomposing the signals, i.e., it could naturally deal with the non-stationarities and non-linearities. Thus, it could be used effectively in extracting the features of the knock from the signals in real-time situations. Current work focuses on various methods that could be adopted for extracting the features of knock within the limitations of EMD and to develop a criterion for detecting the SI engine knock that could lead towards knock detection and control its further occurrence in real-time. The Hilbert Spectrum of the first IMF obtained using EMD is analyzed to study the features of knock. The spectrogram is also obtained by performing Short-Time Fourier Transform (STFT) on the first IMF obtained using EMD. The results are compared to choose the optimal strategy, which could determine the occurrence of knock effectively. The following sections address the details regarding the methodologies used and the results obtained.

2. ENGINE BLOCK VIBRATION ANALYSIS AND SYSTEM CONTROL

In-cylinder pressure and the corresponding engine block vibration signals are taken from the research by Fengrong *et al.* [31-33]. They had captured the signals from 4 cylinders, 4-stroke, in-line SI engine. The ignition timing is advanced to induce knock. Two DYTRAN - 621B40 [31-33] accelerometers were mounted on the engine block (nearby cylinders 2 and 4) to capture the vibrations with a sampling frequency of 51,200 Hz. The pressure transducer AVL - GH13Z-31(24) was used to measure in-cylinder pressure signals [31-33]. From the literature, it is noted that the signals generated during knock contain frequencies ranging from 8 kHz to 22 kHz [9]. For better accuracy, the noise needs to be eliminated before analyzing the signals. Denoising is achieved by applying signal filtering techniques using wavelet filters. The use of soft thresholding minimizes the chance of discontinuities in the denoised signal [34]. The Symlet wavelet is used for denoising the signal since it could reduce the phase distortion due to its better symmetry. The denoised signal is then decomposed using EMD to extract the features of knock. The first intrinsic mode function (IMF1) thus acquired bears the characteristics of knock. Hence, in the current work, only the first IMF is used to study the behavior of knock, even though other IMFs also might contain the features of knock due to the

mode mixing that may arise with the use of EMD. This will also help to ensure a simple methodology to timely address the occurrence of a knock with less computation. Hilbert spectrum and spectrogram of IMF1 are obtained to compare its effectiveness in determining the occurrence of knock. The following sections contain additional details about the analysis.

2.1 EMD Algorithm

EMD was developed by N Huang [13] for analyzing non-stationary signals. A signal could be broken down using EMD into various components with gradually changing amplitude and phase [18]. This property enables it to obtain intrinsic patterns at multiple scales without assuming that the signal is harmonic in nature, stationary, etc., as we do in wavelet Transform or Fourier analysis [22]. The iterative process followed in EMD for obtaining the IMFs, called sifting, and the algorithm used for it is as follows [22]:

- Find the locations of all the extrema in the signal (local extrema), $x'(t)$.
- Obtain the lower envelope, $e_{min}(t)$, by interpolating between all the local minima. Similarly, obtain the upper envelope, $e_{max}(t)$, by interpolating between all the local maxima.

Compute the local mean, $m(t)$, from local minima, $e_{min}(t)$, and local maxima, $e_{max}(t)$ obtained.

- Subtract 'local mean' from 'local extrema' to obtain the 'modulated oscillation', $d(t) = x'(t) - m(t)$
- If the modulated oscillation obtained satisfies the stopping criterion, then it is taken as the first IMF, $IMF_m = d(t)$, so that the new local extrema becomes $x'(t) = x'(t) - IMF_m$, else set it as the new local extrema $x'(t) = d(t)$ and start reiterating from step 1. This process is repeated until all the IMFs are obtained, and the residue becomes a monotonic function.

The stopping criterion checks whether the modulated oscillation satisfies the properties of the IMF, which is as follows [13]:

- Either the extrema and the number of zero crossings must be equal, or they can only differ by one.
- The Mean value of the lower/upper envelope at any point should be zero.

Thus, after the sifting process, IMFs are obtained from which instantaneous frequency can be defined. By using EMD, we can have inter-wave frequency modulations to explain the waveform deformation due to non-linear effects and intra-wave frequency modulation to explain the dispersive propagation of waves [13]. Also, the signal that is decomposed using EMD can be reconstructed perfectly [22]. Amidst all these positives, mode mixing and aliasing are its drawbacks. Mode mixing occurs when either one oscillatory mode is present in multiple IMFs or more than one oscillatory mode is present in one IMF [22]. Aliasing is the overlapping of IMF spectra formed due to the sub-Nyquist nature of extrema sampling [20].

2.2 Hilbert Spectrum

The Hilbert Transform offers a special approach to defining the imaginary components, though there are

multiple theoretical ways to do so. The results, thus, obtained will be an analytic function [13]. A signal can be simultaneously represented in the time and frequency domains by using Hilbert Spectrum [18]. This spectrum works well for pinpointing the locations in time and frequency space where the majority of the energy is concentrated. Hence, it can be used as an important tool in determining the occurrence of a knock and the cylinder at which the knock is occurring. As energy will be focused in the high-frequency regions during the knock occurrence, the resulting Hilbert Spectrum will give an intuitive vision of how much energy is localized in the high-frequency range and when it is occurring. Hence, it would be a great choice for non-stationary and non-linear data analysis. However, the simple Hilbert Transform of the denoised vibration signals contains the entire details about the frequency content of a signal, as it may contain more than one oscillatory mode at any instant [35]. Therefore, rather than finding the Hilbert Transform of a complete signal, it is applied to the first IMF obtained after performing EMD. As a result, using the Hilbert Spectrum, we could derive the localized data associated with the signal in the frequency domain. This, in turn, could identify the hidden local data structures that are embedded in the original signal [14]. In the current work, the Hilbert Spectrum of the first IMF obtained using EMD is plotted to study its effectiveness in determining the occurrence of knock.

2.3 Short-Time Fourier Transform

In contrast to the Fourier Transform, Short-time Fourier Transform (STFT) could provide time-localized information about a signal whose frequency varies with time, while the former could only provide time-averaged information about the frequency [36]. Hence, STFT finds application in analyzing non-stationary signals. Moreover, it requires lower computational power. The vibration signal was mapped into a 2-D function of time and frequency by Al-Badour *et al.* [37] using STFT. In STFT, a non-stationary signal is separated into discrete time frames of identical length before being processed using Fourier transform [38]. Hence, any changes occurring in the signal at any instant could be captured in a time frame. However, EMD is more powerful in capturing all the physics of non-stationary non-linear signals than STFT. Therefore, in the current work, we used a combination of EMD and STFT to utilize the advantages of both. STFT is applied on the first IMF that is obtained after performing EMD of the vibration signal to establish the spectrogram. Thus, the advantage of EMD in extracting the features of the knock from the vibration signal can be utilized. At the same time, we will get a meaningful representation of the knock signal in a spectrogram, which is an intensity plot of STFT magnitude over time.

2.4 Knock detection using In-cylinder pressure

To quantify the intensity of knock, the maximum amplitude of pressure oscillation (MAPO) method was used. If the MAPO surges above 0.5 bar, the corresponding cycle is treated as a knocking cycle. While if it is even

higher than 2 bar, it is treated as a strong knock [39]. MAPO is obtained using the following relation [39].

$$MAPO = \max \left| \hat{P} \right|_{\theta_o}^{\theta_o + \delta}$$

Here \hat{P} is the filtered pressure that was obtained after passing the in-cylinder pressure through a band-pass filter between the frequencies 6 – 20 kHz. θ_o is the crank angle corresponding to the initiation of combustion and δ is the duration of combustion.

The effectiveness of representing the knock signals using the Hilbert Spectrum and spectrogram is addressed in the current work and is explained in the following section. Also, the Hilbert Spectrum and spectrogram are compared along with the MAPO to study their effectiveness in classifying the knock based on its intensity.

3. RESULTS AND DISCUSSION

Figures 1 and 2 show the in-cylinder pressure fluctuations with and without the occurrence of knock.[31-33]. EMD was used to decompose the engine block vibration signals that corresponded to the in-cylinder pressure signals shown in Figs. 1 and 2 [31-33]. Figures 3 and 4 show the IMFs obtained on decomposing the vibration signals produced during the presence and absence of knock, respectively. From Fig. 3 and 4, it is clear that vibrations up to 100 g are produced during the SI engine knock, while the maximum amplitude is only 20 g during the absence of knock. Higher amplitudes in the IMF 1 obtained may be concluded as due to the occurrence of knock. The presence of knock could not be determined just by the fluctuation in the amplitudes of the vibration signals, as was the case with the variations in the in-cylinder pressure. There may be other factors also that cause amplitude fluctuations in the engine block vibrations. Therefore, for further analysis and confirmation, we performed investigations using the Hilbert Spectrum and spectrogram to visualize the energy distribution of the signal at various frequency levels.

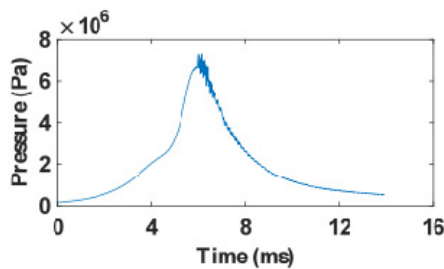


Figure 1: In-cylinder pressure during the occurrence of knock [33].

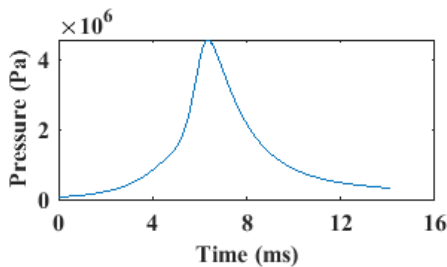


Figure 2: In-cylinder pressure during the absence of knock [33].

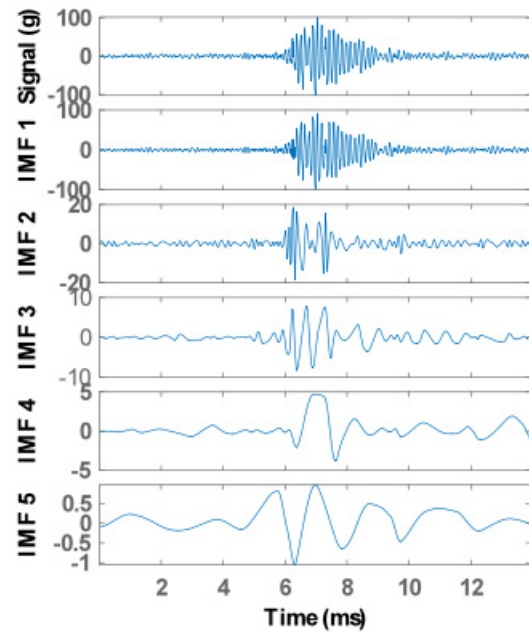


Figure 3: First five IMFs obtained after decomposing the engine block vibration signals using EMD. The signal was captured during the presence of a knock.

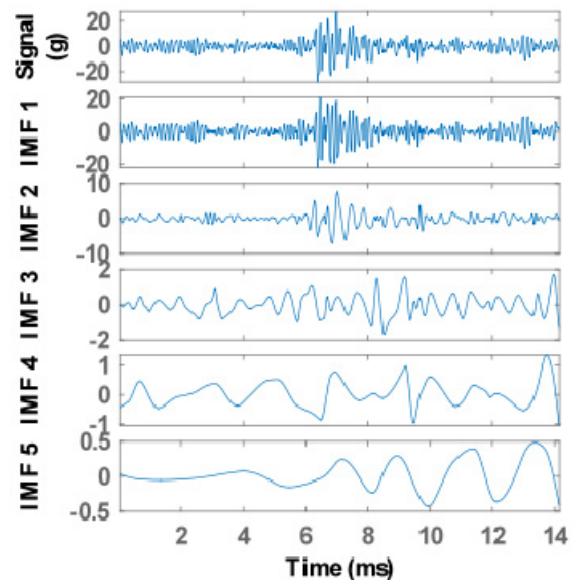


Figure 4: First five IMFs obtained after decomposing the engine block vibration signals using EMD. The signal was captured during the non-knocking cycle.

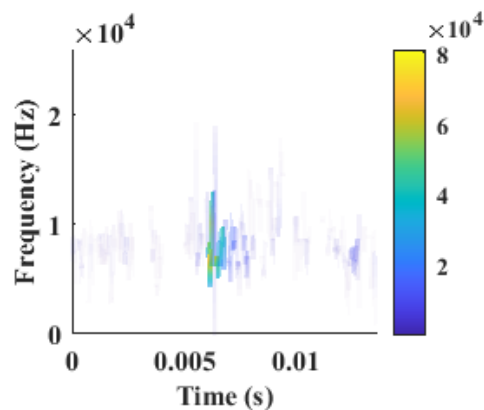


Figure 5: Hilbert Spectrum of the first IMF obtained after performing EMD on the engine block vibration signals produced during the absence of knock.

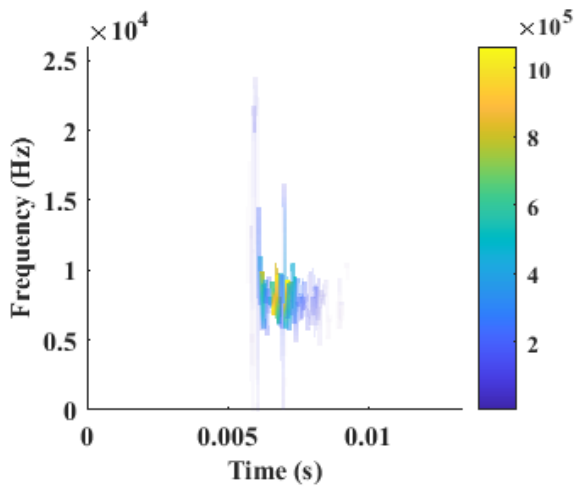


Figure 6: Hilbert Spectrum of the first IMF obtained after performing EMD on the engine block vibration signals produced during the presence of knock.

MAPO is calculated to be 5.46 bar and 0.237 bar corresponding to the in-cylinder pressures shown in Fig. 1 and 2, indicating the presence of a very strong knock and the absence of knock, respectively.

Figures 5 – 8 show the Hilbert spectrum and spectrogram corresponding to the IMF1 obtained during the occurrence of knock and non-knock conditions. From Fig. 6, it is observed that the energy level of the vibration signal falls in the higher frequency ranges, above 20 kHz, during the occurrence of knock. While this was not visible in the Hilbert Spectrum obtained for the normal combustion process (Fig. 5). However, studies revealed that the vibrations are generated when a knock occurs in a range of frequencies between 8 to 22 kHz [9]. From Fig. 5, we can see that the energies of vibration fall in frequencies above 10 kHz even during the normal combustion process. Therefore, it might be difficult to compare the signals for determining the occurrence of knock during the continuous working of an SI engine. To strengthen this, additional analysis of the signals containing data on engine block vibrations generated during combustion in all cylinders in an engine is required.

Alike the Hilbert spectrum, STFT of the IMF 1 was done to obtain the spectrogram, as shown in Fig. 7 and 8. The findings demonstrate that, in contrast, to the normal combustion process, the energy level of the signal is high when a knock occurs. Also, we could see that there are higher energy levels in the frequency range above 20 kHz during the occurrence of knock (Fig. 8). However, we can see that some lower energy level also falls in the high-frequency range during the normal combustion process (in the absence of knock) (Fig. 7). This is not visible in the Hilbert Spectrum of the vibration signals produced during non-knocking cycles. Similar to that of the Hilbert Spectrum, a spectrogram could also be used to identify the time as well as the cylinder in which the knock is occurring. Further investigations are required to find the effectiveness of the Hilbert Spectrum and spectrogram for determining the occurrence of knock, especially when the signal that is to be analyzed is captured from a multi-cylinder engine. This is because the effectiveness of the results may depend on the sample length of the signal and

engine operating parameters like engine speed, the torque developed, etc. Also, the spectrogram or Hilbert Spectrum may change if the sample signal consists of a combination of vibrations produced during the presence and absence of knock.

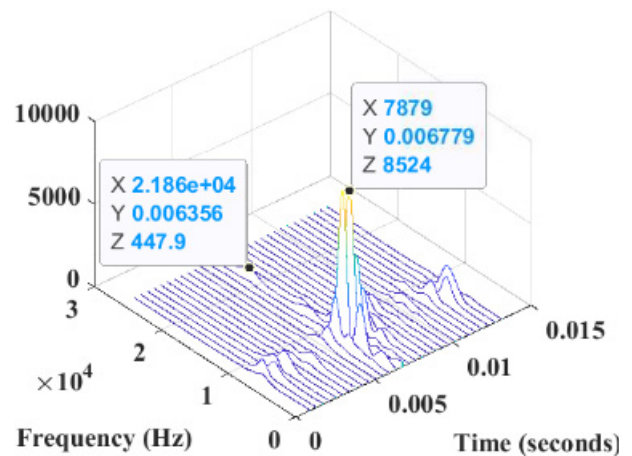


Figure 7: Spectrogram plotted using IMF 1 obtained after performing EMD on the vibration signals taken during the non-knocking cycle.

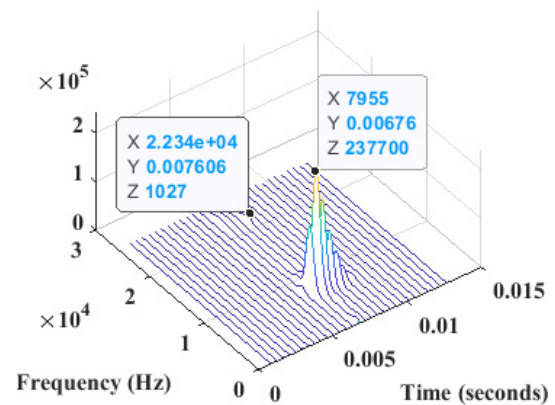


Figure 8: Spectrogram plotted using IMF 1 obtained after performing EMD on the vibration signals taken during the presence of knock.

Figure 9 shows the in-cylinder pressure, its corresponding engine block vibration signal, and IMFs obtained after decomposing the vibration signals using EMD. The signals are captured at 2800 rpm and spark at 28° BTDC [33]. The signal captured is the combination of vibration signals generated during the combustion processes in each cylinder. From Fig. 9, we can see that, in some instances, the amplitude of vibrations goes above 20 g. This may be due to the occurrence of knocking, as seen in Fig. 3. We observe three points where the vibration signals fall above 20g, i.e., around 5 ms, 16.5 ms, and 37.5 ms, respectively. This may be due to the occurrence of knock. However, further investigations are necessary to confirm the same. Similar to the previous analysis, Fig. 10 shows the in-cylinder pressure captured at 4000 rpm and spark at 20° BTDC [33], its corresponding engine block vibration signal, and IMFs obtained after decomposing this vibration signal using EMD. From Fig. 10, we can see that, in some instances, the amplitude of vibrations goes above 20 g, i.e., around 12 ms and 27 ms, which may be due to the occurrence of knock, as discussed previously.

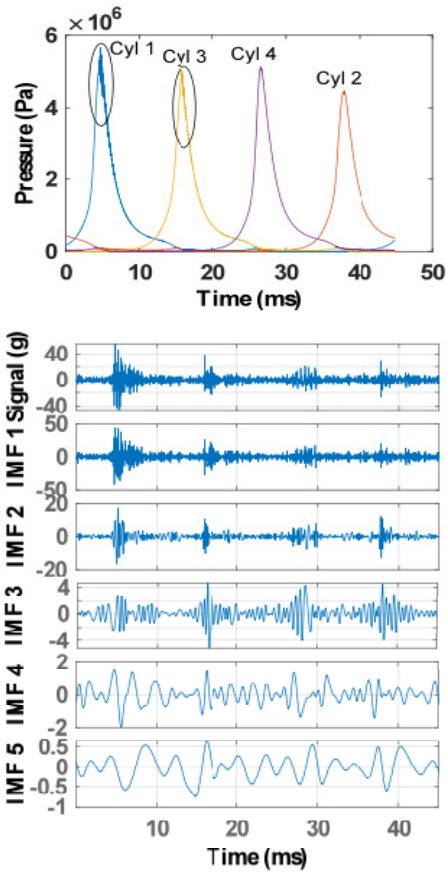


Figure 9: In-cylinder pressure [33] and first five IMFs obtained after decomposing the engine block vibration signals captured at 2800 rpm using EMD.

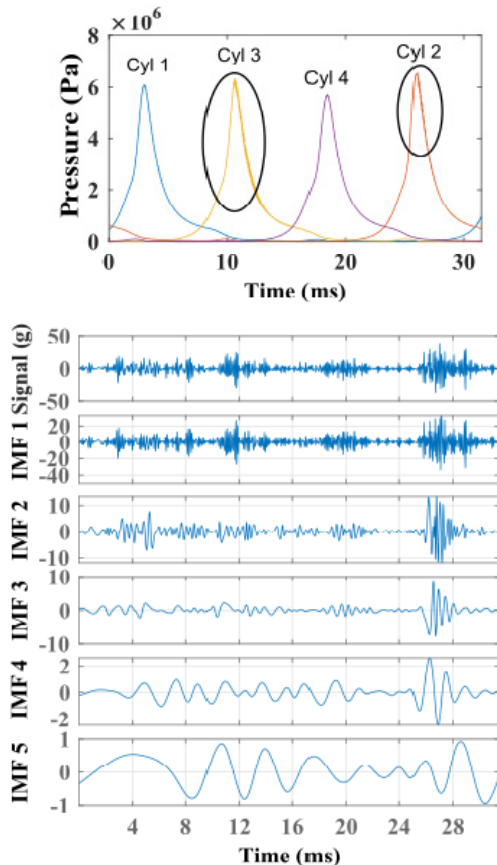


Figure 10: In-cylinder pressure [33] and first five IMFs obtained after decomposing the engine block vibration signals captured at 4000 rpm using EMD.

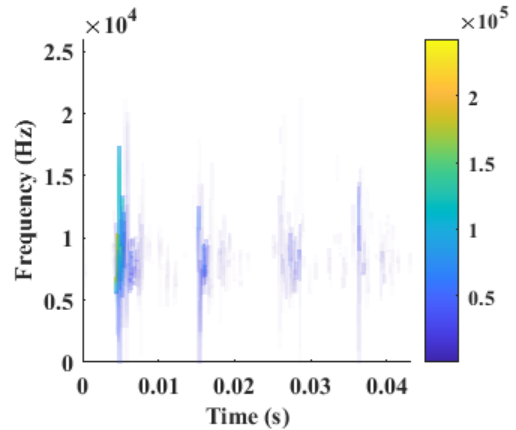


Figure 11: Hilbert spectrum of the IMF 1 obtained after performing EMD on the engine block vibration signals captured at 2800 rpm.

Figure 11 and 12 shows the Hilbert spectrum corresponding to the first IMFs obtained after decomposing the engine block vibration signals shown in Fig. 9 and 10, respectively. In the Hilbert Spectrum obtained, the energy distribution is found to have frequencies above 8 kHz corresponding to the combustion process in each cylinder. Furthermore, the intensity of energy in the higher frequency range is found to be high, around 0.005 seconds and 0.0165 seconds (Fig. 11) and 0.011 seconds and 0.026 seconds (Fig. 12), respectively, for both cases. On comparing the amplitude of the vibrations and their corresponding energy distribution in the Hilbert Spectrum, we could infer that the higher amplitude vibrations corresponding to 5 ms and 16.5 ms shown in Fig. 9 are due to the occurrence of knock. This is due to the higher energy vibration signals with higher frequencies produced during these instances. However, this was absent in the higher amplitude vibrations around 37.5 ms; hence it may not be due to the occurrence of knock.

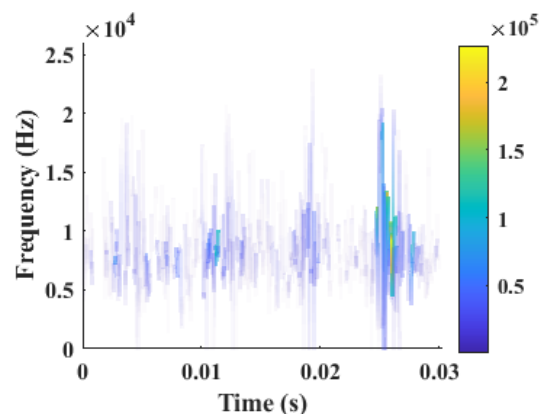


Figure 12: Hilbert spectrum of the IMF 1 obtained after performing EMD on the engine block vibration signals captured at 4000 rpm.

Figure 13 and 14 shows the spectrogram of the first IMFs of the signals given in Fig. 9 and 10. From Fig. 13, it is clear that the vibration energy is maximum at 0.004721 seconds. Also, there are energy levels in the higher frequency regions (above 15 kHz) during the same period. Hence, it could be concluded as a strong knock. The MAPO is corresponding to this in-cylinder

pressure is calculated as 4.94 bar, which is higher than 2 bar, indicating a strong shock. We can also see another peak, smaller in amplitude than the former, at 0.01616 seconds, with some vibration energy falling in the higher frequency range between 10 kHz - 20 kHz; this may be due to a weak knock. The MAPO corresponding to this is calculated to be 1.93 bar, indicating a weak knock since the value is less than 2 bar. For the remaining in-cylinder pressures obtained from cylinders 4 and 2, MAPO is calculated to be 0.28 bar and 0.18 bar, respectively. Since the value is less than 0.5 bar, it is said to be a non-knocking cycle. This was also evident in the energy of vibrations produced corresponding to these regions (shown in Fig. 13), indicating a non-knocking cycle. Similarly, from Fig. 14, we can observe that the energy level is maximum at 0.02589 seconds. We can also observe the energy levels in the higher frequency regions (above 15 kHz) during the same instance, indicating a strong knock. Another peak is observed at 0.01112 seconds with very low energy falling in the higher frequency range between 10 kHz - 20 kHz. However, the vibration energies around 8 kHz are almost the same for both. Therefore, later can also be considered as an indication of a strong knock. MAPO is also calculated using the in-cylinder pressure signals obtained from the corresponding cylinders. They are found to be 2.15 bar and 2.12 bar corresponding to cylinders 3 and 2, respectively, indicating strong knock. This further underlines the inference obtained using the Spectrogram. From the in-cylinder pressure signals corresponding to cylinders 1 and 4, MAPO is calculated to be 0.46 bar and 0.43 bar, respectively, which is less than 0.5 bar, indicating a non-knocking cycle.

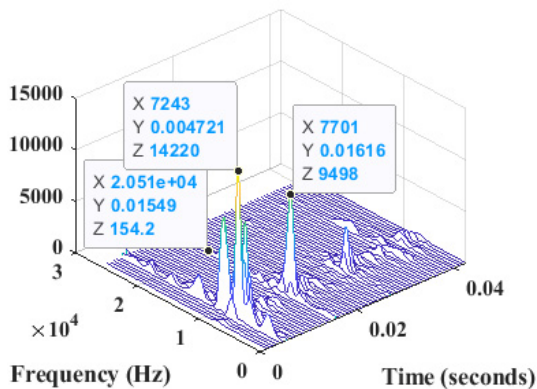


Figure 13: Spectrogram plotted using the IMF 1 obtained after performing EMD on the engine block vibration signals captured at 2800 rpm.

From Figures 11 - 14, it is evident that the maximum value of energy at the higher frequency region is not constant. Hence, proper experiments need to be conducted to find the energy level of the vibrations produced during the knocking cycles that occur in the entire engine operating range for fixing the threshold values. Information regarding the firing order and the engine speed are the only additional data required for identifying the cylinder in which knock is produced. We can also see that in both the Hilbert Spectrum and the spectrogram obtained, energy distribution of the vibration signals is also observed above 10 kHz for both the knock and non-knock conditions. However, the

spectrogram could provide more clarity in the results than that could be conveyed by the Hilbert spectrum.

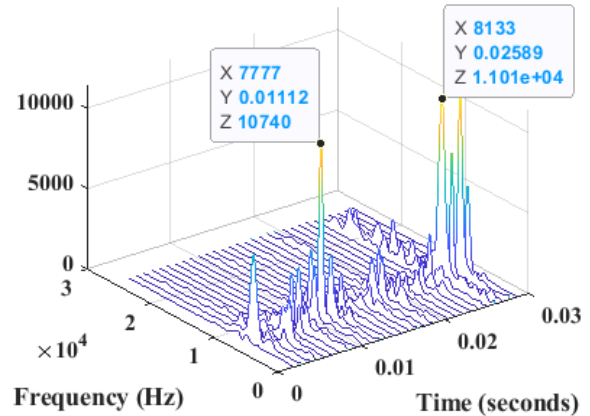


Figure 14: Spectrogram plotted using the IMF 1 obtained after performing EMD on the engine block vibration signals captured at 4000 rpm.

4. CONCLUSION

The engine block vibration signals are decomposed using EMD. The first IMF obtained after decomposing the vibration signals produced while knock occurs evaluated with that obtained during the non-knocking cycle. The higher amplitude fluctuations in the signal could be used to locate the occurrence of knock in the time domain. However, this alone is not sufficient to confirm the occurrence of knock. Hilbert spectrum and spectrogram of the signal are obtained to demonstrate the amplitude fluctuations of the signal in a time-frequency domain. The results show that, during the occurrence of knock, the amplitude of signals falls in the high-frequency region, i.e., above 10 kHz. From the Hilbert spectrum and the spectrogram of the signal, it is clear that both could be used individually to determine the occurrence of knock and also to locate the cylinder at which it is occurring. Further studies reveal that the combination of EMD and STFT (spectrogram) provides more clarity than the Hilbert spectrum obtained after EMD alone. MAPO calculated using the in-cylinder pressures also produced the same inferences as that obtained using the Spectrogram. The current study also shows that the vibration signals captured from the engine block alone could be used to extract the features of knock. This reduces the cost incurred for the sensors and the computational power for using in-cylinder pressure to determine the knock. According to the observations from the current work, the criterion for detecting the presence of knock may be fixed as the first IMF that exceeds the amplitude of 20g and has frequencies above 10 kHz taken together. Furthermore, the energy intensity of vibration signals falling in the higher frequency range above 10 kHz can be analyzed to categorize the knock as strong or weak.

The methodology described in this work could be used to detect the presence of knock with minimum computation. Emphasis was given to identifying a mechanism to determine the knocking cycles so that it could be used in real-time. However, all the features of knock could not be extracted using EMD due to the mode mixing. The findings, however, demonstrate that

spectrograms may accurately capture the vibration signals generated during SI Engine knock in their time-frequency domain, even if some characteristics may have been lost while decomposing.

The pattern of the spectrograms obtained for the several knocking and non-knocking cycles could be used to train the machine learning algorithm. Thus the current work can be extended further to determine the knocking cycles and to take appropriate control measures, such as the reduction in the in-cylinder temperatures using cooled Exhaust Gas Recirculation, etc., to prevent its further occurrence of knock in real-time.

REFERENCES

- [1] John B. Heywood. *Internal combustion engine fundamentals*. McGraw-Hill Education, 2018.
- [2] Antonio Joseph, *et al.*, Approximate analysis of SI engine knocking using wavelet and its control with cooled exhaust gas recirculation, *FME Transactions*, Vol. 44, No. 1, pp. 22–28, 2016.
- [3] A. M. Douaud and P. Eyzat. Four-octane-number method for predicting the anti-knock behavior of fuels and engines, *SAE Transactions*, pp. 294–308, 1978.
- [4] K. Keisuke, *et al.*, *A model widely predicting auto-ignition time for gasoline engines*. Technical report, Tech. report, Toyota Central R&D Labs INC. Mechanical Engineering Department, 2009.
- [5] Vincent Knop, *et al.*, On the use of a tabulation approach to model auto-ignition during flame propagation in SI engines, *Applied Energy*, Vol. 88, No. 12, pp. 4968–4979, 2011.
- [6] Ralph Worret, *et al.*, Application of different cylinder pressure based knock detection methods in spark ignition engines, *SAE Transactions*, pp. 2244–2257, 2002.
- [7] Eric Ollivier, *et al.*, Detection of knock occurrence in a gas SI engine from a heat transfer analysis, *Energy Conversion and Management*, Vol. 47, No. 7-8, pp. 879–893, 2006.
- [8] Laurent Duval, *et al.*, Noise robust spark ignition engine knock detection with redundant wavelet transform, In Proc.: *International Conference on Noise and Vibration*, 2002.
- [9] Ning Li, *et al.*, Determination of knock characteristics in spark ignition engines: An approach based on ensemble empirical mode decomposition, *Measurement Science and Technology*, Vol. 27, No. 4, pp. 045109, 2016.
- [10] Nanshan Li and Mingquan Zhou. Audio denoising algorithm based on adaptive wavelet soft-threshold of gain factor and teager energy operator, In 2008 *International Conference on Computer Science and Software Engineering*, volume 1, pages 787–790. IEEE, 2008.
- [11] Raghuveer Rao, Ajit. B. Bopadikar, *Introduction to theory and applications-wavelet transforms* 2004.
- [12] A. Cohen. Ten lectures on wavelets, cbms-nsf regional conference series in applied mathematics, vol. 61, i. daubechies, siam, 1992, xix+ 357 pp. *Journal of Approximation Theory*, Vol. 78, No. 3, pp. 460–461, 1994.
- [13] Norden E. Huang, *et al.*, The empirical mode decomposition and the Hilbert spectrum for nonlinear and non-stationary time series analysis. *Proceedings of the Royal Society of London. Series A: mathematical, physical and engineering sciences*, Vol. 454, pp. 903–995, 1998.
- [14] Donghoh Kim and Hee-Seok Oh. EMD: A package for empirical mode decomposition and Hilbert spectrum. *The R Journal*, Vol. 1, No. 1, pp. 40–46, 2009.
- [15] Misiti Michel, *et al.*, *Wavelet toolbox for use with Matlab*, user's guide, version 3. The MathWorks.
- [16] Gabriel Rilling, *et al.*, On empirical mode decomposition and its algorithms. In *IEEE-EURASIP workshop on nonlinear signal and image processing*, volume 3, pages 8–11. NSIP-03, Grado (I), 2003.
- [17] K. P. Soman. *Insight into wavelets: from theory to practice*. PHI Learning Pvt. Ltd., 2010.
- [18] Susan Tolwinski. *The Hilbert transform and empirical mode decomposition as tools for data analysis*. Tucson: *University of Arizona*, 2007.
- [19] V. R. Vimal Krishnan and P. Babu Anto. Features of wavelet packet decomposition and discrete wavelet transform for malayalam speech recognition, *International Journal of Recent Trends in Engineering*, Vol. 1, No. 2, pp. 93, 2009.
- [20] Zhaohua Wu and Norden E. Huang. Ensemble empirical mode decomposition: A noise-assisted data analysis method. *Advances in adaptive data analysis*, Vol. 1, No. 1, pp. 1–41, 2009.
- [21] Matijević DV, Popović VM. Overview of modern contributions in vehicle noise and vibration refinement with special emphasis on diagnostics, *FME Transactions*, Vol. 45, No. 3, pp. 448-458, 2017.
- [22] Danilo P. Mandic, *et al.*, Empirical mode decomposition-based time-frequency analysis of multivariate signals: The power of adaptive data analysis. *IEEE signal processing magazine*, Vol. 30, No. 6, pp. 74–86, 2013.
- [23] Oumar Niang, *et al.*, Partial differential equation-based approach for empirical mode decomposition: application on image analysis, *IEEE Transactions on Image Processing*, Vol. 21, No. 9, pp. 3991–4001, 2012.
- [24] Kim J. In-cylinder pressure based engine knock classification model for high-compression ratio, automotive spark-ignition engines using various signal decomposition methods. *Energies*. 2021 May 26;14(11):3117.
- [25] Ofner AB, Kefalas A, Posch S, Geiger BC. Knock detection in combustion engine time series using a theory-guided 1-D convolutional neural network approach. *IEEE/ASME Transactions on Mechatronics*. 2022 Feb 8;27(5):4101-11.
- [26] Rosas, M., Amador, G. "Knock detection method for dual-fuel compression ignition engines based on block vibration analysis." *SAE International Journal of Engines* 14.2 (2021): 199-210.

- [27] Ismail, M.M., et al. "Engine knock detection for a multifuel engine using engine block vibration with statistical approach." *MethodsX* 8 (2021): 101583.
- [28] Ilić, Z., Rašuo, B., Jovanović, M., Janković, D.: Impact of Changing Quality of Air/Fuel Mixture during Flight of a Piston Engine Aircraft with Respect to Vibration low Frequency Spectrum, *FME Transactions*, Vol. 41 No.1, pp. 25-32, 2013
- [29] Ilić, Z., Rašuo, B., Jovanović, M., Jovicčić, S., Tomić, Lj., Janković, D., Petrašinović, D.: The Efficiency of Passive Vibration Damping on the Pilot Seat of Piston Propeller Aircraft, *Measurement*, Vol. 95, pp. 21-32, 2017
- [30] Ilić, Z., Rašuo, B., Jovanović, M., Pekmezović, S., Bengin, A., Dinulović, M.: Potential Connections of Cockpit Floor – Seat on Passive Vibration Reduction at Piston Propelled Airplane, *Technical Gazette*, Vol.21, No.3, pp. 471-478, 2014
- [31] Fengrong Bi, *et al.*, Knock detection in spark ignition engines base on complementary ensemble empirical mode decomposition-Hilbert transform. *Shock and Vibration*, 2016.
- [32] Fengrong Bi, *et al.*, Knock feature extraction in spark ignition engines using EEMD-Hilbert transform. Technical report, SAE Technical Paper, 2016.
- [33] Fengrong Bi, *et al.*, Development of a novel knock characteristic detection method for gasoline engines based on wavelet-denoising and EMD decomposition. *Mechanical Systems and Signal Processing*, Vol. 117, pp. 517–536, 2019.
- [34] A. Kabir, C. Shahnaz: Denoising of ECG signals based on noise reduction algorithms in EMD and wavelet domains, *Biomedical Signal Processing and Control*, Vol. 7, No. 5, pp. 481–489, 2012.
- [35] Steven R. Long, *et al.*, The Hilbert techniques: An alternate approach for non-steady time series analysis. *IEEE Geoscience Remote Sensing Soc. Lett*, Vol. 3, pp. 6–11, 1995.
- [36] Nasser Kehtarnavaz. *Digital signal processing system design: LabVIEW-based hybrid programming*, Elsevier, 2011.
- [37] F. Al-Badour, *et al.*, Vibration analysis of rotating machinery using time–frequency analysis and wavelet technique, *Mechanical Systems and Signal Processing*, Vol. 25, No. 6, pp. 2083–2101, 2011.
- [38] Wahyu Caesarendra and Tegoeh Tjahjowidodo, A review of feature extraction methods in vibration based condition monitoring and its application for degradation trend estimation of low-speed slew bearing, *Machines*, Vol. 5, No. 4, pp. 21, 2017.
- [39] Lasocki J, Engine knock detection and evaluation: A review. *Zeszyty Naukowe Instytutu Pojazdów*, Vol. 109, No. 5, pp. 41-50, 2016.

NOMENCLATURE

\hat{P}	Filtered pressure having frequencies between 6-20 kHz is the
$x'(t)$	Local extrema
$e_{min}(t)$	Lower envelope
$e_{max}(t)$	Upper envelope
$d(t)$	Modulated oscillation

Greek symbols

θ_o	Ignition timing
δ	Duration of combustion

ACRONYMS AND ABBREVIATIONS

HUCR	Highest Usable Compression Ratio
EMD	Empirical Mode Decomposition
IMFs	Intrinsic Mode Functions
EEMD	Ensemble Empirical Mode Decomposition
STFT	Short-Time Fourier Transform
MAPO	Maximum Amplitude of Pressure Oscillation
BTDC	Before Top Dead Centre

ВИБРАЦИЈЕ БЛОКА МОТОРА - ИНДИКАТОР КУЦАЊА У СИ МОТОРУ

В.К.А. Цозеф, Т. Гирешкуманан

Фактори који утичу на почетак куцања имају значајан утицај на то колико добро СИ мотор ради. Дакле, ефикасност у одређивању почетка и контроли детонације је кључни фактор у побољшању перформанси СИ мотора. Овај рад даје увид у улогу вибрација блока мотора у одређивању појаве детонације коришћењем емпиријске деком–позиције и краткорочне Фуријеове трансформације. Да би се разумело понашање вибрација у условима нормалног сагоревања и куцања, сигнали вибрације блока мотора се анализирају и упоређују са флукуацијама притиска у цилиндру. Карактеристике куцања се издвајају из вибрацијских сигнала блока мотора коришћењем емпиријског режима декомпозиције. Прва тако добијена функција унутрашњег мода (ИМФ) се користи за генерисање Хилбертовог спектра за откривање појаве детонације. Слично, краткорочна Фуријеова трансформација се такође изводи на првом ИМФ-у за добијање спектрограма. Налази недвосмислено показују да се веће варијације фреквенције производе када дође до куцања. Ови резултати такође указују на то да се комби–нација емпиријског модуса декомпозиције и крат–котрајне Фуријеове трансформације може ефикасно користити за одређивање појаве детонације.